RSC Advances

ROYAL SOCIETY OF CHEMISTRY

www.rsc.org/advances

Journal Name

ARTICLE

Hybrid aminopolymer-silica materials for efficient CO_2 adsorption

Pedro López-Aranguren[a], Santiago Builes[b], Julio Fraile[a], Ana López-Periago[a], Lourdes F. Vega[c], Concepción Domingo*[a]

Received 00th January 20xx,
Accepted 00th January 20xx

DOI: 10.1039/x0xx00000x

www.rsc.org/

The present work focuses on the development of a new eco-efficient chemical method for the polymerization of aziridine to hyperbranched polyethyleneimine (PEI) into mesoporous silica by using compressed CO_2 as a solvent, reaction medium and catalyst. PEI was *in situ* grafted into MCM-41 and silica gel substrates, with pore diameters of 3.8 and 9.0 nm, respectively. The optimal polymerization conditions were found by varying the reaction pressure (1.0-10 MPa), temperature (25-45 ºC) and time (20-400 min). The thermal stability analysis indicated that aminopolymers chains were covalently attached on the amorphous silica surface. The described compressed CO_2 route for the synthesis of high amine content hybrid products (6–8 mmolNg^{-1}) is a very fast method, with processing times in the order of few minutes even at very low working pressures (1.0 MPa), being a step forward in the design of efficient hybrid aminopolymer nanocomposites for CO_2 capture. The adsorptive behavior of the prepared hybrid materials was experimentally established by recording the N_2 (-196 ºC) and CO_2 (25, 50 and 75 ºC) adsorption isotherms. Results were compared to molecular simulation studies performed using Grand Canonical Monte Carlo for either N_2 or CO_2 adsorbed on amino modified MCM-41, thus helping to elucidate the predominant PEI configuration present in the functionalized materials.

1 Introduction

Polymers bearing side functionalities that are capable of reacting with other molecules are attractive to be used in adsorptive processes. Particularly, polymers having amino functionalities have been proposed for applications in CO_2 adsorption after being grafted on porous substrates.[1] Ordered mesoporous silica are excellent candidates as solid supports, because of their high surface area, high pore volume, tunable pore size and good thermal and mechanical stability. Molecular amines, silanes, monomers and polymers are used in the synthesis of these polymer nancocomposite solid-support adsorbents with applications in CO_2 capture[1]. Among the polymer materials used to functionalize porous supports, dendrimers and hyperbranched polymers have drawn more interest because of their flexible architecture and reactive versatility[2]. This article makes emphasis on discussing a facile, fast and green method developed for the functionalization of mesoporous silica substrates with hyperbranched polymers synthetized *in situ* using compressed CO_2, meanwhile, the unique properties and potential applications of the resultant nanocomposites are also analyzed.

The current concern about anthropogenic CO_2 impact on global climate change has resulted in the design of different procedures for CO_2 capture and storage (CCS)[1]. Even if the necessary reduction in the CO_2 anthropogenic emissions required to avoid irreversible changes cannot be accomplished without a massive switch to non-fossil energy sources, the emissions can be moderated by adsorbing and recovering CO_2 from point sources. As a consequence, removal of CO_2 from diluted gaseous streams has become a requirement in the chemical industry. Indeed, the concept of separating CO_2 from flue gas streams started in the 1970s, with processes based on chemical absorption using aqueous alkanol amines[3]. This process has been widely used for CO_2 separation in food and beverages industries, among others. However, the amount of CO_2 to be adsorbed and separated in the context of CCS poses a challenge to this and other technologies, being a research area of high technological interest. Nowadays, the developed procedures described for the separation of CO_2 from a gas mixture can be summarized as: the already mentioned absorption in liquid aqueous amines, reaction with calcium-based materials, separation with membrane technology, ionic liquids[4,5] and sorption into micro and mesoporous solid substrates.[6,7] Although the latter is one important alternative procedure for CCS, a massive industrial implementation of this technology requires the design of sorbents with high stability, capacity and selectivity.

The family of aminosilica porous solid sorbents is one of the most promising candidates to design a potentially less-energy-intensive CO_2 separation technology than the use of aqueous amines.[8] For these hybrid sorbents, the proper selection of a suitable silica support, together with an efficient NH_x-containing organic, is of vital importance. Regarding the support, amorphous mesoporous silicas may be the answer to design highly efficient adsorbents, being particularly important silica materials with ordered pore space in one and three-dimensional structures.[9] Regarding the amino moiety, the first adsorbents were developed by physical impregnation in a substrate of different amine-containing organic polymers, mainly poly(ethyleneimine) (PEI). In the 1990s, NASA designed a regenerable CO_2, sorbent consisting of

[a] Instituto de Ciencia de Materiales de Barcelona (ICMAB-CSIC), Campus de la UAB. 08193 Bellaterra, Spain. E-mail: conchi@icmab.es
[b] Grupo de Investigación DDP, Universidad EAFIT. Medellín, Colombia
[c] Alya Technology & Innovation. Centre de Promoció Empresarial. C/ Tres Creus, 236. 08203 Sabadell, Barcelona, Spain

PEI deposited into polymethyl methacrylate, as part of the life support system used to clean the air from the crew compartment in aircrafts, submarines, and spacecraft vehicles.[10] Following the classification suggested by Hicks *et al.*[11] for supported amine sorbents (class 1, 2 and 3), physical impregnation leads to class 1 adsorbents. More recently, high-capacity class 1 molecular basket sorbents have been developed using mesoporous MCM-41 substrate impregnated with PEI dissolved in toluene.[12,13] Class 2 adsorbents are typically prepared through the grafting of aminosilanes on the silanols of the silica surface.[14,15] Class 3 adsorbents are prepared by the polymerization of aminomonomers, e.g., aziridine, directly on the support surface, thus creating covalent bonds.

The synthesis of class 3 hybrid materials is here addressed from a new and more sustainable perspective. In organic solvents, the ethyleneimine or aziridine monomer is converted into a highly branched PEI polymer by ring-opening polymerization in the presence of an acid catalyst. The first example of aziridine polymerization initiated on surface was performed on previously aminosilylated silica substrates, using the primary amine to initiate the polymerization.[16] However, it was later showed that the hydroxyl groups on the silica surface are also able to initiate the ring-opening polymerization of aziridine by themselves when using acetic acid as a catalyst.[11,17,18] Current methods designed to graft hyperbranched polyamines on inorganic surfaces require organic solvents, acid catalysts, high temperatures, and/or long reaction times.[19] Only recently, the use of organic solvents and catalysts to obtain tethered surface-grown PEI has been avoided by using either vapor-phase transport[20] or supercritical fluid[21] technologies. Although the vapor-phase transport is a free-solvent process that uses the acid silica support to induce the nucleophilic ring-opening polymerization of aziridine, it still requires long reaction times and high temperatures. Conversely, a fast and low temperature process based on the use of supercritical CO_2, both as a reaction media and as a catalyst, was outlined in a previous communication.[21] This work focuses on the variables influencing the supercritical or compressed CO_2 polymerization process to obtain mesoporous class 3 adsorbents with grafted PEI. The procedure used for the synthesis was analyzed in terms of pressure, temperature and reaction time. The study is extended to the analysis of two different mesoporous forms of silica, silica gel and MCM-41, in order to analyze the influence of pore size and pore interconnectivity on both PEI loading and CO_2 adsorption, and to search for the best operating conditions. It was shown that this process occurs under very soft experimental conditions, even below supercritical CO_2 conditions. A detailed characterization of the adsorptive behavior of the obtained class 3 materials was performed regarding the N_2 and CO_2 gravimetric uptakes. In addition to the experimental measurements, computational models for MCM-41 grafted with PEI were evaluated for N_2 and CO_2 adsorption and compared to experimental data. Results obtained from Grand Canonical Monte Carlo (GCMC) simulations allowed a better understanding of the predominant configuration present in the functionalized materials.

2 Materials and methods

2.1 Materials

Aziridine was kindly supplied by Menadiona S.A. Two different porous supports were used: silica gel (CC, Cleancat Iberamigo S.A.) and MCM-41 (ACS Materials). The mesoporous MCM-41 was first activated in distilled water at 100 ºC for 1 h to increase the surface silanol density. Both supports were dried in an air-oven at 120 ºC overnight before use. CO_2 (99.999%, Carburos Metálicos S.A.) was used as a solvent.

2.2 Equipment and procedure

The supercritical process was carried out in a 100 mL high-pressure autoclave (TharDesign) running in batch. Two single-crystal sapphire windows, placed 180º apart in the reactor body, allowed a visual follow-up of the process taking place inside the reactor. The vessel was charged with 0.3 g of silica, enclosed in a cylindrical cartridge made of 0.45 µm pore filter paper, and 1 mL of liquid aziridine, avoiding the physical contact between substrate and monomer.[22] The vessel was then slowly pressurized with CO_2 up to a pressure (P) between 1 and 10 MPa. The polymerization was carried out at a temperature (T) of either 25 or 45 ºC during a period of time (t) of 20 or 400 min under stirring at 150 rpm. *Caution: Aziridine is a reproductive effecter and a tumorigenic agent and should be handled with care. Moreover, due to its self-reactive character with CO_2, the process must be performed with proper personal protection equipment.* At the end of each experiment, the reactor was depressurized and allowed to cool down to room temperature. A distinctive experiment was performed at 6 MPa and 45 ºC for 20 min, giving place to the reference samples: r-MCM and r-CC for MCM-41 and CC substrates, respectively. In this run, the PEI obtained as a residue at the bottom of the reactor after supercritical processing was recovered and characterized (sample PEI_{CO2}). When necessary, as-synthesized samples were outgassed at 120 ºC for 2 h to eliminate remaining CO_2 in the form of carbamate.[23]

2.3 Chemical characterization

Fourier transform infrared (FTIR) spectra of samples were recorded on a Perkin-Elmer Spectrum One instrument to confirm the presence of the polymer in the treated materials. PEI loadings were determined by thermogravimetric analysis (TGA), performed under N_2 flow with a TGA Instrument Q5000 IR. In some selected samples, TGA data was corroborated by elemental analysis of C, H, and N using a Flash EA2000 Thermo Fisher Sci. Samples were first heated at 120 ºC for 2 h. Each analysis was performed using triplicate parallel samples. An Applied Biosystems Voyager 6214 time-of-flight mass spectrometer equipped with a matrix-assisted laser desorption/ionization source (MALDI-ToF) was used to estimate the molecular weight of the synthesized PEI_{CO2} polymer.

The percentage of primary amines in the PEI grafted onto the r-MCM sample was estimated throughout derivatization with 4-nitrobenzaldehyde (4-NBZ), following a reported procedure.[24] For this purpose, a weighted amount (*ca.* 50 mg) of the functionalized substrate was immersed into 20 mL of anhydrous ethanol containing excess (30-40 mg) of 4-NBZ and stirred at 50 ºC under inert atmosphere for 24 h. After the corresponding condensation reaction took place, the suspension was centrifuged for 5 min at 4500 rpm to recover the solid, which was further re-suspended in methanol and sonicated for 1 min. The sonication process was repeated two more times using dichloromethane and methanol sequentially. The sample was then dried under vacuum and quantitatively hydrolyzed in 50 mL of water containing acetic acid (0.1 mL). The obtained suspension was heated and stirred under reflux for 24 h. The aqueous phase acquired a yellowish color indicating the release of the 4-NBZ. The yellow solution was separated from the powder by centrifugation. Finally, the

concentration of regenerated 4-NBZ was measured with an UV–vis spectrophotometer (Varian Cary 5) at a λ of 267 nm.

2.4 Textural characterization

Textural characteristics of raw and treated substrates were studied by low temperature N_2 adsorption–desorption at -196 ºC (ASAP2000 Micromeritics). Prior to measurements, samples were outgassed under reduced pressure at 120 ºC for 20 h. The specific surface area was determined by the BET method. The mesopore volume (P_v) was calculated using the BJH method from the adsorption branch of the isotherm.

2.5 CO_2 adsorption characterization

Sorption isotherms of CO_2 were obtained in the interval 0-100 kPa using a Micromeritics ASAP 2020 analyzer. Prior to the measurements, samples were outgassed under reduced pressure following the same procedure than for N_2 adsorption. A circulator bath containing heated oil was used to obtain CO_2 isotherms at different temperatures. Isotherms were collected at 25, 50 and 75 ºC. The study of the CO_2 adsorption/desorption cyclic behavior was performed using a microelectronic recording balance (IMS HP HT microbalance, based on a magnetically coupled Rubotherm GmbH microbalance) with a cell of 100 mL. Measurements were carried out at atmospheric pressure under a total flow of 200 cm^3min^{-1}. The samples were first dried and decarbamated by passing N_2 at 105 ºC for 180 min. Then, they were cooled down to the desired adsorption temperature. The CO_2 uptake for the prepared sorbents and the further regeneration process were analyzed under the principles of temperature swing adsorption. CO_2 adsorption was carried out at 50 ºC in a mixture of dry CO_2 (10 v%) and N_2 for 90 min, while CO_2 desorption was performed at 105 ºC under a flow of pure N_2. A minimum of 10 cycles were applied to each sample and 20 cycles were applied to the reference products.

2.6. Computational analysis

Ordered MCM-41 was chosen for the computational study. The pristine porous matrix and the functionalized materials were simulated following a previously described methodology.[25] The amorphous silica structure generated by this procedure provides a sufficiently realistic model of the materials hydroxylated surface for further functionalization, as demonstrated previously by silane grafting.[26] In the simulated PEI grafting procedure, it was assumed that the functionalization was solely driven by surface reaction. Predefined polymer chains were covalently bonded to a selected number of silanols on the support surface. Three lineal (Nl chains) and two branched (Nb chains) low molecular weight PEI chains were used in the simulations (Fig. 1a). Options 2Nl, 3Nl and 4Nl correspond to linear simple models containing two, three and four primary and/or secondary amine units. Options 3Nb and 5Nb represent branched polymers involving also tertiary amines. Each of these structures was assumed to exist exclusively inside the porous material during simulation, that is, each simulation contained solely one kind of the polymeric chains grafted to the MCM-41 surface. Although this is a simplistic model of the complex structure likely found inside the pores, it allows isolating the effects of each type of configuration on the adsorption behavior of the functionalized materials. Samples containing a similar loading than the experimental r-MCM material (4.6 $mmol_N$ per gram of sample corresponding to 5.3 $mmol_N$ per gram of dry and empty substrate) were constructed.

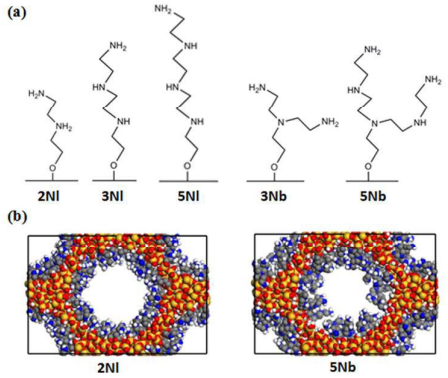

Fig. 1 PEI chains: (a) configurations used in the simulations, and (b) generated models for MCM-41 functionalized with either the 2Nl or 5Nb chain.

By fixing the uptake, the number of silica surface silanols substituted by a polymer unit varies depending on the chosen configuration. The calculated amount of chains grafted on the surface were 1.8, 1.2, 0.9, 1.2 and 0.7 grafted chains per nm^2 for 2Nl, 3Nl, 4Nl, 3Nb and 5Nb configurations, respectively. The polymeric chains were built segment by segment, starting from the silanol oxygen on the silica. Fig. 1b shows a visual comparison of the models of the MCM-41 substrate grafted with configurations 2Nl and 5Nb. In configuration 2Nl the small polymer chains are densely covering the silica surface, whereas in configuration 5Nb the chains are less densely packed on the surface.

For MCM-41 with the different grafted chains, N_2 and CO_2 adsorption simulations were performed by the GCMC method, following a published procedure.[27] The soft-SAFT equation of state was used to relate the pressure of the bulk fluid to the chemical potential of the adsorbate.[28] The silica atoms were kept rigid while the amine chains were allowed to move. Using this methodology, the N_2 physisorption process was first studied as a function of the applied pressure. Next, simulated CO_2 adsorption isotherms at 25 and 50 ºC were generated by considering chemisorption at low CO_2 pressure and physisorption at all pressures. Chemisorption was simulated by simultaneously adding during functionalization a predefined number of carbamate and protonated aminopolymer chains.[29] A 35 and 25 % efficiency for the CO_2-amine reaction was assumed for experiments at 25 and 50 ºC, respectively.

3 Results and discussion

The two different supports scrutinized in this work are constituted of amorphous silica. MCM-41 has a periodic pore structure organized in 1D arrays of non-intersecting hexagonal channels, whereas the CC silica gel has a 3D interconnected pore network. MCM-41 and CC are mesoporous, with pore diameters of 3.8 and 9 nm, and large surface areas of 1127 and 440 m^2g^{-1}, respectively. Both are polar substrates with a hydroxyl surface density of 4-6 $OHnm^{-2}$. PEI is a water soluble cationic polymer that can take both linear and branched forms. The random branched structure is commonly produced by acid-catalyzed polymerization of aziridine in liquid solution (Fig. 2a).[30] In this case, the polymerization is activated by aziridine protonation, followed of nucleophilic attack

by a second aziridine molecule. In the presence of an acid catalyst, this monomer is converted into a highly branched polymer with *ca.* 25:50:25 % of primary:secondary:tertiary (1º:2º:3º) amine groups.[31] Under dry conditions, only 1º and 2º amines are efficient in adsorbing CO_2. Hence, the design of an efficient CO_2 adsorbent implies the determination and control of the distribution of the amine types in the PEI chains.

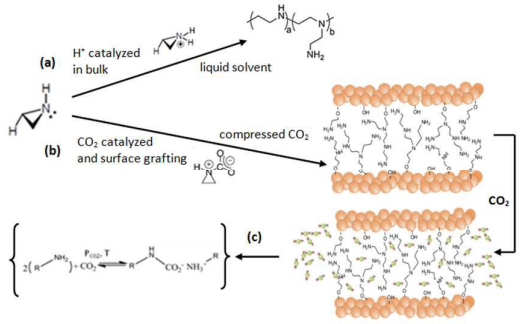

Fig. 2 Ring-opening polymerization of aziridine: (a) acid-catalyzed, and (b) CO_2-catalyzed; and (c) reaction of carbamate formation by CO_2 addition to a PEI system.

Table 1. Experimental conditions and TGA measured PEI loading values, expressed as both weight percentage and specific molar density respectively, estimated volume occupied by loaded PEI, and deviation of amine loading calculated with respect to the averaged loading values for the reference r-MCM and r-CC samples.

Sample	P MPa	T ºC	t min	load wt%	load $mmol_N$ g^{-1}	load cm^3_{PEI} g^{-1}	dev %
MCM-41	-	-	-	-	-	-	-
r-MCM	6.0	45	20	20	4.6/4.1*	0.18	<10
1-MCM				24	5.5	0.22	
2-MCM				19	4.4/3.9*	0.17	
3-MCM				20	4.6	0.18	
4-MCM				24	5.6/5.2*	0.23	
5-MCM	10	45	20	34	8.0	0.32	60
6-MCM	2.5	45	20	35	8.1	0.32	62
7-MCM	1.0	45	20	35	8.2	0.33	64
8-MCM	6.0	25	20	26	6.0	0.24	20
9-MCM	9.0	25	20	22	5.1	0.20	2.2
10-MCM	2.5	25	20	17	4.0	0.16	-23
11-MCM	6	45	400	16	3.7	0.15	-26
CC	-	-	-	-	-	-	-
r-CC	6.0	45	10	12	2.9/2.8*	0.12	<10
1-CC				13	3.0	0.12	
2-CC				10	2.4	0.10	
3-CC				11	2.5	0.10	
4-CC				14	3.3/3.2*	0.13	
5-CC	10	45	20	18	4.3	0.17	54
6-CC	2.5	45	20	22	5.2	0.21	86
7-CC	1.0	45	20	23	5.4	0.22	93
8-CC	6.0	25	20	13	3.1	0.12	11
9-CC	9.0	25	20	10	2.4	0.10	-14
10-CC	2.5	25	20	8.1	1.8	0.07	-36
11-CC	6.0	45	400	16	3.8	0.15	35

* Data obtained from elemental analysis

The ring opening polymerization can also be initiated by a Lewis acid, such as CO_2 (Fig. 2b).[32] For unsubstituted aziridine, it has been proved that CO_2 is not significantly incorporated to the polymer chain, even under compressed CO_2.[33] Contrarily, under similar experimental conditions, substituted aziridines react with CO_2 to give copolymers of polyurethane.[34,35] Besides being a catalyst for aziridine polymerization, supercritical CO_2 has shown to be an efficient solvent for the surface modification and functionalization of micro and mesoporous materials.[36,37] Hence, the present work explores the possibility of using this medium for simultaneously producing the polymerization and the grafting of PEI on the internal surface of mesporous silica by using compressed CO_2 both as a solvent and catalyst. Experimental conditions of each run are shown in Table 1, together with some products characteristics. Mesoporous aminosilica adsorbents with different amine loadings were prepared using the supercritical method by varying the applied pressure (from 2.5 to 10 MPa), temperature (25 or 45 ºC) and reaction time (20 or 400 min).

3.1 Molecular identification of grafted compounds

FTIR spectroscopy was used to monitor the presence of the polymer in the hybrid products. Fig. 3 shows the spectra of the reference CC and MCM-41 as-synthesized materials. For comparison, the spectra of PEI_{CO2} as-synthesized and after CO_2 evacuation at 120 ºC are also included. Relevant infrared bands were assigned following data compiled by Bacsik *et al.*[38] on amine-modified silica contacted with CO_2.

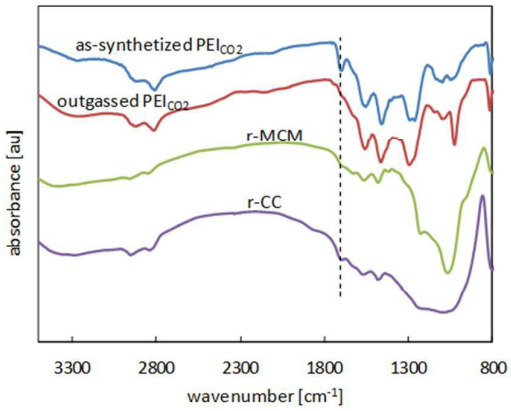

Fig. 3 FTIR spectra of as-synthesized reference products and residual PEI_{CO2} sample as-synthesized and after heating at 120 ºC for 2 h. The vertical line indicates the peak of carbamate at *ca.* 1700 cm^{-1}.

For the as-synthesized and outgassed PEI, the bands corresponding to the CH_x bending vibrations are observed at 2950 and 2820 cm^{-1}, and the characteristic peak corresponding to –NH functional group appears at 1465 cm^{-1}. The band corresponding to N–C stretching emerges at 1565 cm^{-1}. The spectrum of the grafted PEI also exhibits the characteristic absorption peaks of polyamines involving N-C, -NH and CH_x vibrations. For the as-synthesized aminosilicas and PEI_{CO2} samples, carbamate formation during synthesis in the CO_2 rich atmosphere was evidenced by the presence of the band corresponding to C=O stretching at *ca.* 1700 cm^{-1}.

3.2 Polymer molecular weight and structure

The process of PEI polymerization in conventional liquid solutions occurs in a homogeneous mixture, which allows the formation of high-molecular weight PEI, typically within the range of 20000–50000 Da. Contrarily, for tethered surface-grown PEI, the high density of chains grafted on the internal surface interferes with the propagation of hyperbranched tree-like structures, resulting in the decrease of the PEI apparent molecular weight. Thus, silica grafted polyamines prepared by the acid catalyzed liquid-phase method

have molecular weights in the order of 4500-6500 Da,[18] which decreases to 250-2000 Da in hybrids obtained by the vapor phase transport technique.[20]

The molecular weight of PEI synthesized *in situ* and grafted onto the porous supports is difficult to ascertain. Instead, in this work the molecular weight of the bulk polymer PEI_{CO2} was estimated from the generated MALDI-ToF mass spectrum (Fig. 4a). Even if the aminopolymer grown in bulk may differ from the grafted polymer, this measurement was considered to be qualitatively representative of the molecular weight of the loaded PEI. Short PEI chains with a molecular weight distributed between 130 and 1000-2000 Da were found for the PEI_{CO2} sample. These values are in the order of those found for compounds prepared using the vapor phase technique.[20] The ring-opening polymerization of aziridine in a compressed CO_2 atmosphere is an exothermic process occurring at high reaction rates.[39] The quick heat release vaporizes the monomer resulting in a vapor cloud visually observed at low pressures (*ca.* 1 MPa). Hence, the process has initially a homogeneous vapor phase reaction, where the monomer and initiator, in this case the Lewis acid CO_2, are intimately mixed.

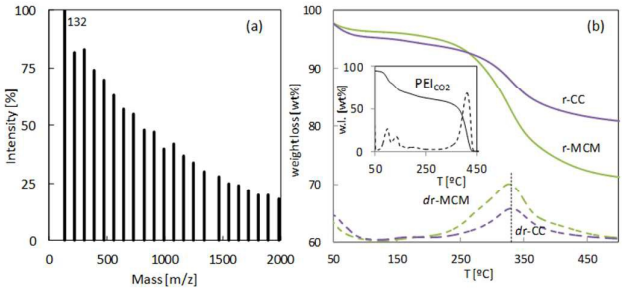

Fig. 4 Thermal decomposition of: (a) PEI_{CO2} MALDI-ToF mass spectrum, and (b) TGA profiles and first derivative (*d*) and PEI_{CO2}.

During polymerization, the system becomes rapidly heterogeneous once the growing oligomeric chains reach a critical molar mass that exceeds the solubility limit in the compressed CO_2 phase. Polymer precipitation would significantly reduce the molecular weight of the recovered PEI_{CO2} product. During the observed vaporization step, the silica channels are impregnated with the linear monomer or short oligomers. These chains are then grafted on the silica surface and begin to grow. It is hypothesized that the grafted polymer would have a still lower molecular weight than the PEI_{CO2}, since aminopolymer growth and branching are restricted by the available pore space inside the silica support.

Whatever catalytic method is used, aziridine forms a hyperbranched aminopolymer that contains a mixture of 1º, 2º and 3º amines. In general, decreasing the molecular weight of PEI increases the content of 1º and 2º respect to 3º amines.[40,41] In this work, the amount of 1º amines for the grafted species was estimated for the reference MCM-41 sample by derivatization with 4-NBZ and further UV analysis, giving a value of *ca.* 20 %. For amino-functionalized particles or flat surfaces, this analytical method has demonstrated to be quantitative.[16] However, for mesoporous supports, the 4-NBZ flow through the charged channels would have spatial restrictions and not all the 1º amino groups would be accessible for the imine reaction. Thus, the value of 20 % was likely an underestimation. Similar values, although slightly higher (25-30 %), have been reported for 1º amines in PEI chains grafted onto silica by the acid catalyzed liquid method.[18]

PEI polymer can grow on the silica surface with different morphologies, including linear and hyperbranched. The C, H, N elemental analysis performed on the reference and PEI_{CO2} samples was used to envisage feasible degrees of branching. Measured C:H:N weight ratios were compared with calculated values from the molecular weight for the five different PEI morphologies in Fig. 1a, the aziridine unit chain ($-CH_2CH_2NH_2$) and the hyperbranched 25:50:25 polymer. Note that these molecules have different ratios of 1º:2º:3º amines. Theoretical and measured C:H:N data were normalized by N weight. For N=1, the theoretical ratio of C for all the tested PEI chain structures is 1.71. The theoretical calculations indicate that enhancing the degree of branching, i.e., increasing the percentage of 2º and 3º amines, reduces the H ratio. Thus, for the monomer the calculated H ratio is 0.43, for the 2Nl chain 0.39, for the 3Nl, 4Nl and 3Nb structures 0.38, and for the 5Nb compound 0.37. The H ratio is further reduced to 0.36 for the hyperbranched polymer. The first general observation for the evaluated experimental samples with elemental analysis was a relatively higher C content with respect to the value of 1.71. Measured C ratios were of 2.09, 1.90 and 2.01 for r-MCM, r-CC and PEI_{CO2} samples, indicating that some CO_2 was incorporated to the system during synthesis, either forming part of the polymer chain as urethane linkages[42] or, most likely, as carbamate. Measured H ratios for the reference hybrid products were 0.39 and 0.4 for r-MCM and r-CC samples, respectively. These H values match molecules with low degree of hyperbranching, as expected for the grafted low molecular weight polymers. The PEI_{CO2} sample has a C:H:N ratio of 2.01:0.35:1, being the measured low H value indicative of a highly hyperbranched product formed in an environment with no sterical restrictions under CO_2 catalytic conditions.

3.3 Loading and reproducibility

The loading data presented in Table 1, expressed as a percentage in weight of PEI, was obtained by TGA measurements. Representative weight loss curves for the reference hybrid materials are shown in Fig. 4b. The decomposition of the grafted PEI occurs in the temperature range 200-400 ºC. The weight loss observed below this range was associated with desorption of CO_2 and moisture. The PEI weight values grafted on the MCM-41 support were in the range of 20-35 wt%, while smaller values were obtained for the CC matrix, in the order of 10-20 wt%. Loading values were recalculated from the TGA weight percentages as mmol of nitrogen per gram of sample [$mmol_N g^{-1}$] by inference of a stoichiometric ratio of aziridine units.[18] The measured loadings are in line with reported data of grafted PEI in SBA-15 and MCM-41 synthesized by different methods.[18,20,43] For comparison, the loading for some products synthesized under the conditions of the reference sample was also analyzed by elemental analysis (Table 1). TGA and elemental analysis loadings were similar, although TGA values were slightly higher, particularly for the highly loaded MCM-41 support.

Aided by CO_2, the ring-opening polymerization of aziridine results in a violent exothermic reaction that can create aminopolymers uncontrollably. Indeed, at *ca.* 1 MPa, the instantaneous formation of a dense vapor cloud due to fast polymerization was visually observed inside the reactor, coupled with a simultaneous temperature increase of *ca.* 5 ºC. Hence, to investigate whether the uncontrolled but constrained polymerization was reproducible, the typical batch designed at 6 MPa and 45 ºC (20 min) was repeated four times (samples r-, 1-, 2- and 4- in Table 1), while two similar supports added in different

cartridges were functionalized side by side in the same batch (samples 2- and 3- in Table 1). For the MCM-41 samples, the averaged loading value was 5.0 $mmol_N g^{-1}$, with minimum and maximum values of 4.4 and 5.6 $mmol_N g^{-1}$. For the CC samples, the averaged loading value was 2.9 $mmol_N g^{-1}$, with minimum and maximum loading values of 2.4 and 3.3 $mmol_N g^{-1}$. For these four groups of samples, the standard deviations for the loading were 0.53 and 0.37 for MCM-41 and CC products, respectively, which corresponded to less than 10 wt% of the loading in both cases (Table 1). Moreover, the loadings of the two different samples synthesized in the same batch were very similar.

3.4 Influence of processing parameters on loading

In Fig. 5, PEI loading values are represented for MCM-41 and CC hybrid products for each set of studied experimental conditions (Table 1). In general, higher specific amino density values were obtained by grafting the polymer onto the MCM-41 support than onto the CC matrix. This behavior has been previously described in the literature,[22,43] and rationalized in regards to the superior surface area of supports with smaller pores, which are not counteracted by the favorable mass transport properties of materials with larger pore diameter.[44,45]

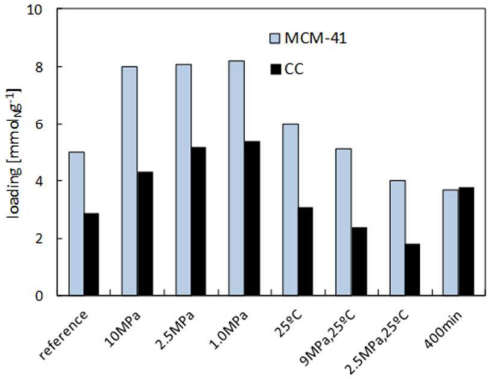

Fig. 5 Loading, expressed as mmol of incorporated nitrogen per unit weight, as a function of the experimental conditions.

The influence of the process variables P, T and t in the loading was here assessed. Results are discussed in comparison to the mean loading value of the reference materials. From these values, a deviation percentage was calculated for the rest of the prepared products (Table 1). Under similar temperature and reaction time, the influence of the pressure in the loading values was noticeable. For both substrates, the PEI uptake increased by more than 50 % when increasing the pressure from 6 to 10 MPa (samples 5-MCM and 5-CC). Surprisingly, the increase in the loading was similar or even higher by decreasing the pressure from 6 MPa to values as low as 2.5 (samples 6-MCM and 6-CC) or 1 MPa (samples 7-MCM and 7-CC). Conversely, the influence of the temperature was less significant. Decreasing the temperature from 45 to 25 ºC at 6 (samples 8-MCM and 8-CC) or 9 MPa (samples 9-MCM and 9-CC), increased the estimated loading around 10-20 %; but this variation was close to the previously measured standard deviation in the reference materials. The low influence of the temperature can be linked to the high exothermic character of the ring-opening polymerization reaction. The heat released by the violent polymerization likely develops a large localized temperature increase, independent of the external heating, at least in the temperature range studied. The simultaneous reduction of the pressure to 2.5 MPa and the temperature to 25 ºC (samples 10-MCM and 10-CC) slightly reduced the loading.

The influence of increasing the reaction time from 20 to 400 min was reverse for both substrates (samples 11-MCM and 11-CC). This observation can be rationalized on the basis of the different pore size and pore interconnectivity of both substrates. On one side, the MCM-41 material has a hexagonal array of 3.8 nm diameter parallel channels. Modification of this substrate *via* 20 min of supercritical polymerization saturates the pores and extending the processing time was likely to be useful only to extract non-grafted chains, thus reducing the measured loading. On the other side, the silica gel CC substrate, with an interconnected network of large mesopores (8.8 nm), can increase the loading values by diffusion of monomers and growth of the polymer chains.

3.5 Thermal stability

The thermal stability of aminosilica hybrid materials is critical, since it has a direct impact on the temperature range in which materials can be used and the frequency of replacement of the adsorbents. The thermal stability of the prepared samples was discussed based on the TGA profiles recorded for the reference samples shown in Fig. 4b. PEI_{CO2} featured three-step weight decays in the temperature interval of 50-500 ºC (inset in Fig. 4b). Up to 150 ºC, the weight loss was attributed to water and CO_2 desorption (*ca.* 25 wt%). The polymer began to decompose above 150 ºC and *ca.* 35 wt% of its dry weight was gradually lost up to 375 ºC. Above 375 ºC, the degradation rate sharply increased, indicating a different decomposition process. For grafted PEI, the sharp weight loss at high temperatures (200-400 ºC) was the most evident feature of the thermograph. The first derivative curves (*dr*-MCM and *dr*-CC in Fig. 4b) indicated a maximum weight loss rate occurring at *ca.* 330 ºC. Grafted PEI in mesoporous ordered silica prepared using the liquid or the vapor diffusion technique decomposed with the maximum occurring at 200[46,47] or 250 ºC,[20] respectively. Hence, significant decomposition for samples prepared using compressed CO_2 was shifted more than 100 ºC to the right, indicating notable higher thermal stability than similar products in the literature.

3.6 N_2 adsorption and textural properties

The pore volume of the studied substrates, before and after PEI loading, was obtained from the temperature N_2 adsorption isotherms. Assuming a density of 1.07 gcm^{-3} for the grafted PEI, similar to the density of commercial PEI, the volumetric loading [$cm^3_{PEI}g^{-1}$] was calculated for the different achieved grafting densities (Table 1). In each case, the volume occupied by the aminopolymer was significantly smaller than the open pore volume of the bare substrates, as determined by N_2 adsorption isotherms (0.92 and 0.89 cm^3g^{-1} for MCM-41 and CC, respectively). Hence, potentially, all added polymer could be located into the pores. For the hybrid products, the pore volume decreased as a function of the grafting density. However, the decrease was more noticeable for MCM-41 than for CC functionalized products, having the former a higher percentage of grafted PEI. Fig. 6a,b shows the N_2 adsorption isotherms of the raw adsorbents, those of the medium loaded reference samples (r-MCM and r-CC) and those of highly loaded samples obtained at 10 MPa (5-MCM and 5-CC).

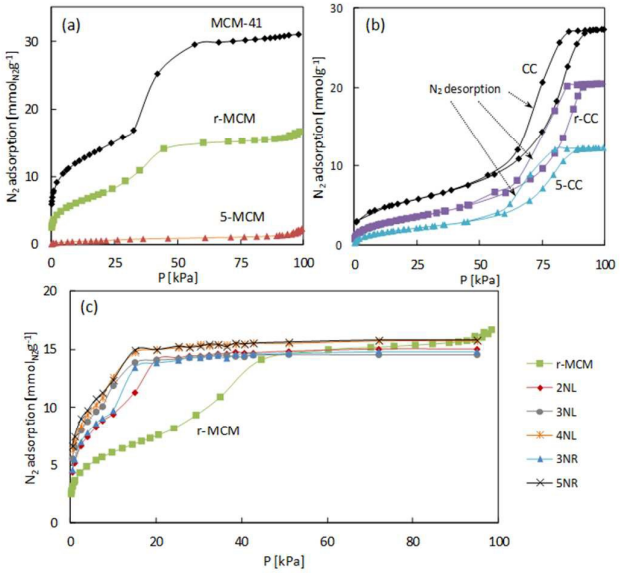

Fig. 6 N_2 adsorption/desorption isotherms for: (a) pristine MCM-41 and selected r-MCM and 5-MCM treated samples, (b) pristine CC and selected r-CC and 5-CC treated samples, and (c) r-MCM sample compared with simulated profiles applying the different PEI chains in Fig. 1a to the modeled MCM-41 substrate.

The adsorption isotherm for MCM-41 with pores of around 4.0 nm, which is type IV in the IUPAC classification, shows two distinct features: a sharp capillary condensation step at a relative pressure of 0.4 and no hysteresis between the adsorption and desorption branches (Fig. 6a).[48] The adsorption at very low relative pressure, P/Psat, is due to monolayer adsorption of N_2 on the walls of the mesopores and does not represent the presence of any micropores. However, in the case of materials with pores larger than 4.0 nm, as it is the case of the CC silica gel studied in this work, a change from a reversible type IV isotherm (MCM-41 in Fig. 6a) to a typical type IV isotherm with hysteresis loop of the H1 type (Fig. 6b) occurs.

The r-MCM sample showed an adsorption isotherm that still preserves significant mesoporosity, while the 5-MCM product exhibited an almost flat isotherm with insignificant N_2 adsorption (Fig. 6a). PEI grafting into CC matrix led to a decrease in the void space for both the r-CC and 5-CC samples, but the overall shape of the adsorption isotherms remained unchanged (Fig. 6b). Comparing both substrates, for the medium loaded MCM-41 reference product (20-25 wt% of PEI), the pore volume was reduced in *ca.* 50 % after PEI grafting, while this decrease was only of 20 % for r-CC (10-14 wt%). The fundamental mesoporous structure remained intact after *ca.* 25 wt% PEI loading for both substrates. By increasing the loading to values of 35 wt% in samples 5-MCM and 7-MCM, the pore volume sharply decreased to residual values of 0.05-0.07 cm^3g^{-1}, indicating pore blocking for N_2 adsorption. For these samples, theoretically, still a large part of empty volume is available, since the grafted PEI only occupied 0.32-0.33 cm^3g^{-1} of the total 0.92 cm^3g^{-1} empty volume. However, the N_2 molecules cannot easily diffuse to access all the pore volume due to the presence of polyamines grown near or in the pore mouths, and likely also to the steric hindrance caused by the formed carbamates in the CO_2 atmosphere.

Using the GCMC simulation method described in the experimental section, the shape of the isotherm for the MCM-41 support has been shown to be analogous to the experimental bare material, particularly up to a N_2 adsorption pressure of 50 kPa.[23,24] The adsorption isotherms were here modeled for the MCM-41 substrate loaded with 4.6 $mmol_Ng^{-1}$ of each one of the PEI chains shown in Fig. 1a. Fig. 6c shows that the N_2 uptake at 100 kPa was similar for both experimental (r-MCM sample) and modeled materials. However, the shape of the isotherm was different in each case. N_2 saturation was attained at lower pressures in the simulated than in the experimental measurements. This difference can be explained as an artifact resulting from the low temperature of the experimental measurements. At -196 ºC, the polymeric grafted chains are in a solid state resulting in N_2 diffusion barriers. On the contrary, in GCMC simulations the molecules are adsorbed in the available pore space without considering the trajectory, thus avoiding diffusion issues.

3.7. CO_2 adsorption, diffusion and kinetics

CO_2 adsorption at low pressures in aminosilicas occurs mainly by chemisorption. The CO_2-amine interaction is described as an exothermic acid-base reaction.[49-51] For 1º and 2º amines under dry conditions, the reaction is proposed to occur in two stages: first, one amine reacts with one molecule of CO_2 by a zwitterion mechanism, followed by base catalyzed deprotonation *via* a second amine group to form a stable carbamate ion (Fig. 2c).[52] The reaction is reversible, allowing for the adsorbent to be regenerated by thermal, vacuum or pressure swing adsorption cycles. For the amino functionalized materials two mutually divergent effects are expected to arise by rising the CO_2 adsorption temperature. On the one hand, gas uptake due to both physical and chemical adsorption decreases, as they are exothermic processes, but on the other hand, the NH_x-CO_2 reaction kinetics, the mobility of PEI polymeric chains and the CO_2 diffusion through filled pores are all favored.

In general, class 1 sorbents involving impregnated PEI exhibit a higher CO_2 uptake than class 3 with grafted PEI, due to the higher nitrogen content usually measured in class 1 materials. For mesoporous systems involving MCM-41,[12,44] MCM-48[42] and SBA-15 [44,53-55] impregnated with PEI in *ca.* 50 wt%, the reported CO_2 uptakes, under a flow of diluted CO_2 and after a fixed period of time, are in the interval of 1.5-2.9 $mmol_{CO2}g^{-1}$. However, these high CO_2 adsorption values are only reached by performing the adsorption at temperatures higher than 75 ºC, since the viscous nature of the impregnated high molecular weight PEI hinders CO_2 diffusion at lower temperatures.[54,56,57] In an attempt to reduce diffusion difficulties, PEI impregnated layered silica materials have been proposed as sorbents for CO_2.[58] The main drawback of class 1 adsorbents is the lack of thermal stability, since polymers are only deposited on the pores. Polymer bonding to the silica surface in class 3 adsorbents significantly improves the thermal stability. For applications related to CO_2 adsorption, grafted hyperbranched aminopolymers are often preferred as modifiers *vs*. aminosilanes, since they have a higher amino density.[59,60]

CO_2 adsorption isotherms CO_2 adsorption isotherms were used as the primary metric to evaluate the performance of synthesized hybrid samples. The temperature dependence of the carbamation reaction is the key factor to design a temperature swing adsorption process. Hence, adsorption isotherms were recorded at 25, 50 and 75 ºC in a pure CO_2 atmosphere up to 100 kPa. The adsorption capacity of the MCM-41 hybrid products was superior to that of CC samples (Table 2), reflecting the higher loading measured for the former materials. Indeed, the equilibrium CO_2 adsorption values of 0.6-0.9 $mmol_{CO2}g^{-1}$ found for the CC hybrid products prepared in this work were in line with the values found in the literature, while

the MCM-41 functionalized samples showed an extraordinarily high adsorption capacity, in the order of 0.9-1.6 $mmol_{CO2}g^{-1}$.

Table 2 Measured CO_2 adsorption from the isotherms at different temperatures and CO_2 uptake in the adsorption/desorption first cycle.

Sample	load mmol g^{-1}	T ºC	CO_2 ad* $mmol_{CO2}$ g^{-1}	CO_2 uptake† $mmol_{CO2}$ g^{-1}
r-MCM	4.6	25	1.56	
		50	1.11	0.44
		75	0.91	
5-MCM	8.0	25	0.89	
		50	1.27	0.95
		75	1.43	
r-CC	2.9	25	0.75	
		50	0.58	0.30
5-CC	4.3	25	0.84	
		50	0.66	0.68

* Measured from the CO_2 adsorption isotherms; † Measured after contacting during 90 min with a flow of diluted CO_2

In the studied temperature range, CO_2 adsorption isotherms for MCM-41 and CC pristine supports showed insignificant adsorption at low pressures and only a low physisorption capacity (< 0.2 $mmol_{CO2}g^{-1}$) at 100 kPa.[61] Contrarily, functionalized samples had a high initial CO_2 adsorption at very low pressures, which corresponds to the contribution of the chemical reaction. Due to the exothermic nature of the CO_2 reaction with amines, the adsorption capacity is expected to decrease with an increase in temperature. Accordingly, this is the behavior observed for the medium loaded reference samples measured at different temperatures (Table 2, Fig. 7a and b for r-MCM and r-CC samples, respectively). N_2 experiments showed that these samples do not have important restrictions regarding diffusion, since after functionalization a relatively large amount of pore volume still remains open (Table 1). At 25 ºC, the highly loaded 5-MCM sample showed a CO_2 adsorption value of only 0.89 $mmol_{CO2}g^{-1}$, which is nearly half the capacity of the r-MCM sample (1.56 $mmol_{CO2}g^{-1}$), and this occurs despite having an amine loading that is twice the value of the reference material (Table 2). Furthermore, the behavior with temperature of the 5-MCM sample was also peculiar (Fig. 7c).

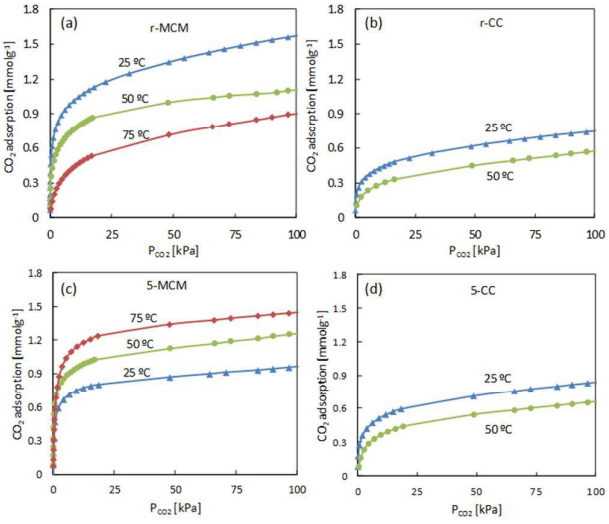

Fig. 7 CO_2 adsorption isotherms of PEI grafted into the porous substrates at different temperatures (25-75 ºC) for samples: (a) r-MCM, (b) r-CC, (c) 5-MCM, and (d) 5-CC.

In this case, the CO_2 adsorption increased with the temperature in the studied interval, indicating a kinetically (diffusion)-controlled process. It is worth mentioning that the almost total loss of pore volume previously measured for this sample by N_2 adsorption (Table 1) did not entirely hinder CO_2 adsorption, even at low adsorption pressures (Fig. 7c). This apparent contradiction is related to the much higher temperature used for the CO_2 adsorption measurements (25 to 75 ºC) compared to the -196 ºC used for N_2 adsorption, temperature at which PEI chains are expected to behave as rigid materials. For the highly loaded 5-CC sample, the variation in the CO_2 adsorption with temperature was as expected for an exothermic adsorption process (Fig. 7d), i.e., decreased with temperature increase from 25 to 50 ºC (Table 2), which fundamentally worked against the formation of carbamate molecules. The CC support has a pore diameter twice the size of MCM-41 and it did not presented diffusion barriers even at high amine loadings, which was also reflected in the N_2 adsorption isotherm (Fig. 6).

Experimental CO_2 adsorption isotherms at 25 and 50 ºC for the functionalized MCM-41 materials were compared to the corresponding models obtained for each one of the different PEI chains in Fig. 1 grafted on the silica surface. The CO_2 adsorption values of experimental (r-MCM sample) and the five model materials were in the same order of magnitude and the isotherms had a similar shape (Fig. 8), corroborating the assumption employed in the simulation, related to the chemical reaction occurring at low pressure. A close observation indicates that the chain configurations that better match the experimental values are those corresponding to 3 aziridine units, in either the linear (3Nl) or branched (3Nb) configuration. This result agrees with the MALDI-ToF analysis, in which the maximum peak intensity corresponds to 3 (132 Da) repeating units (CH_2CH_2NH) in the protonated PEI_{CO2} (Fig. 4a).

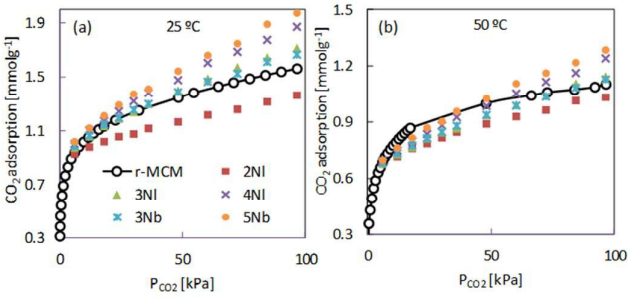

Fig. 8 CO_2 adsorption isotherms for the reference r-MCM product and the five simulated materials using the chains in Fig. 1a and the MCM-41 support, at (a) 25 ºC, and (b) 50 ºC.

CO_2 uptake and adsorption rate CO_2 sorption and separation carried out in realistic conditions is a dynamic process involving both adsorption, with simultaneous chemisorption and physisorption, and desorption processes. Moreover, it is usually performed in the presence of other light gases.[62] In this work, the study of CO_2 adsorption-desorption cycles was performed using a microelectronic magnetic recording balance under a flow of dry CO_2 (10 v%) and N_2 at 50 ºC. This analysis is important to evaluate the influence of the PEI loading in the adsorption kinetics, since diffusion of CO_2 can be drastically retarded in highly loaded samples, thus making the material not practical for further applications. The samples were first dried and decarbamated by passing N_2 during 180 min at 105 ºC. By examining the first

recorded curve in the microbalance adsorption/desorption cycles, the values of CO_2 uptake were estimated after 90 min of passing a diluted flow of CO_2 through the medium (r-MCM an r-CC) and highly loaded (5-MCM and 5-CC) samples (Table 2). CO_2 uptake values were, in general, smaller than the adsorption values obtained at equilibrium. The main differences were found for the samples involving the MCM-41 matrix, reflecting its inherent diffusion barriers, which increased the time necessary to reach the equilibrium.

At 50 ºC, CO_2 uptakes for the highly loaded samples were twice as much as the values of the reference products (Table 2). The CO_2 uptake of the supercritically prepared materials was compared with published uptake data for grafted PEI synthesized using the organic-liquid or the vapor approach. For mesoporous MCM-48 (5.2 $mmol_N g^{-1}$)[63] and SBA-15 (7.2 $mmol_N g^{-1}$)[20] the reported CO_2 uptake are 0.3 and 0.9 $mmol_{CO2} g^{-1}$ at 50 ºC (50 min) and 25 ºC (6 h), respectively. Drese *et al.*[18,43] reported higher CO_2 uptake values than those for PEI grafted on SBA-15 of different pore sizes, but their results were obtained under humid conditions, which favors the formation of carbonate, instead of carbamate increasing CO_2 uptake considerably.

CO_2 adsorption/desorption cycles showed that the uptake measured in the first cycle was successfully maintained after 20 cycles, in accordance with previous studies.[21,64] The cyclic profiles can be divided into three different steps: fast adsorption occurring in empty adsorbents, slow adsorption occurring close to equilibrium, and desorption. The influence of the PEI loading in the adsorption and desorption rates is shown in Figure 9a and b for samples involving MCM-41 and CC, respectively.

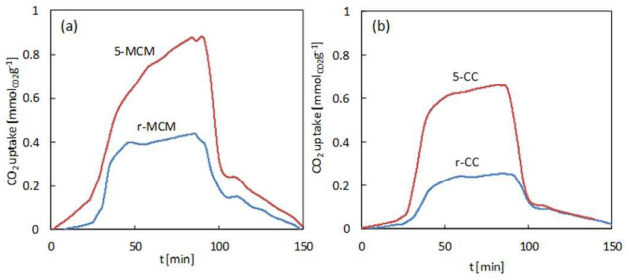

Fig. 9 Comparison of the first adsorption/desorption profiles for: (a) samples r- and 5-MCM, and (b) r- and 5-CC.

Under similar experimental conditions, adsorption rates in the fast adsorption region were similar for r-MCM, r-CC and 5-CC. This rate was significantly slower for sample 5-MCM. The reason for this behavior is linked with the larger pore diameter of CC silica gel with respect to MCM-41 support, which would facilitate gas diffusion even for the highly loaded 5-CC sample. Contrarily, the observed slow adsorption rate in the 5-MCM reflects the described diffusional barriers for this sample. Indeed, significant adsorption in the slow adsorption region was only observed for this sample. Analyzing the desorption rate, faster rates were obtained for the highly PEI loaded samples, regardless of the support used.

4 Conclusions

Different mesoporous silicas were successfully grafted with hyperbranched polyethileneimine by ring opening polymerization of aziridine in compressed CO_2, even when working at low pressure (1.0 MPa), temperature (45 ºC) and a reaction time in the order of few minutes. A high degree of synthesis reproducibility was attained. The CO_2 is here used as solvent and catalyst. High amine loadings (6–8 $mmol_N g^{-1}$) were obtained with a percentage of primary amines of *ca.* 20 %. The polymer forms covalent bonds with the silica, conferring high thermal stability to the hybrid product. The use of the molecular simulation models allowed a better understanding of the predominant configuration present in the functionalized materials, based solely on the adsorption behavior of the experimental materials. The prepared amino silica hybrid products exhibit relatively high CO_2 adsorption capacity, good selectivity and fast adsorption and desorption rates. The CO_2 adsorption isotherms in the 25-75 ºC temperature interval showed that synthesized sorbents can be regenerated under mild conditions, such as those used in temperature swing adsorption.

Acknowledgements

The financial support of the Spanish government under project CTQ2014-56324 is gratefully acknowledged. Additional support has been provided by the Generalitat of Catalonia under Projects 2014SGR377 and 2014SGR1582. A. López-Periago acknowledges the RyC-2012-11588 contract. Menadiona S.A. is acknowledged for the free provision of the aziridine monomer.

References

1 J. Gibbins and H. Chalmers, *Energy Policy*, 2008, **36**, 4317-4322.
2 J-T. Sun, Ch-Y. Hong and C-Y. Pand, *Polym. Chem.*, 2011, **2**,998-1007
3 A. B. Rao and E. S. Rubin, *Environ. Sci. Technol.*, 2002, **36**, 4467-4475.
4 E.D. Bates, R,D. Mayton, I. Ntai, J.H. Davis Jr., *J. Am. Chem. Soc.*,2002, **124**, 927-928.
5 R. Giernoth, *Angew. Chem. Int. Ed.,* 2010, **49**, 2834-2839.
6 S. Choi, J. H. Drese and C. W. Jones, *Chem. Sus. Chem.*, 2009, **2**, 796-854.
7 Q. Wang, J. Luo, Z. Shong and A. Borgna, *Energy Environ. Sci.*, 2011, **4,** 42-55.
8 A. Samanta, A. Zhao, G. K. H. Shimizu, P. Sarkar and R. Gupta, *Ind. Eng. Chem. Res.*, 2012, **51**, 1438-1463.
9 Z. Wu and D. Zhao, *Chem. Commun.*, 2011, **47**, 3332-3338.
10 S. Satyapal, T. Filburn, J. Trela and J. Strange, *Energy & Fuels*, 2001, **15**, 250-255.
11 X. Xu, C. Song, J. M. Andresen, B. G. Miller and A. W. Scaroni, *Energy & Fuels*, 2002, **16**, 1463-1469.
12 X. Xu, C. Song, J. M. Andresen, B. G. Miller and A. W. Scaroni, *Microp. Mesop. Mater.*, 2003, **62**, 29-45.
13 M. W. McKittrick and C. W. Jones, *Chem. Mater.*, 2003, **15**, 1132-1139.
14 P. López-Aranguren, J. Fraile, L. F. Vega and C. Domingo, J. *Supercrit. Fluids*, 2014, **85**, 68- 80.
15 H. Jin-Kim, J. Ho-Moon and J. Won-Park, *J. Coll. Interf. Sci.*, 2000, **227**, 247-249.
16 C. Ok-Kim, S. Ju-Cho and J. Won-Park, *J. Coll. Interf. Sci.*, 2003, **260**, 374-378.
17 J. C. Hicks, J. H. Drese, D. J. Fauth, M. L. Gray, G. G. Qi and C. W. Jones, *J. Am. Chem. Soc.*, 2008, **130**, 2902-2903.
18 J. H. Drese, S. Choi, R. P. Lively, W. J. Koros, D. J. Fauth, M. L. Gray and C. W. Jones, *Adv. Funct. Mater.,* 2009, **19**, 3821-3832.
19 P. Kubisa and S. Penczek, *Prog. Polym. Sci.*, 1999, **24**, 1409-1437.

20 W. Chaikittisilp, S. A. Didas, H-J. Kim and C. W. Jones, *Chem. Mater.*, 2013, **25**, 613-622.
21 P. López-Aranguren, L. F. Vega and C. Domingo, *Chem. Commun.*, 2013, **49**, 11776-11778.
22 P. López-Aranguren, J. Saurina, L. F. Vega and C. Domingo, *Microp. Mesop. Mater.*, 2012, **148**, 15-24.
23 M. Schladt, T. P. Filburn and J. J. Helble, *Ind. Eng. Chem. Res.*, 2007, **46**, 1590-1597.
24 J. H. Moon, J. W. Shin, S. Y. Kim and J. W. Park, *Langmuir*, 1996, **12**, 4621-4624
25 S. Builes and L. F. Vega, *J. Phys. Chem. C*, 2012, **116**, 3017-3024.
26 S. Builes, P. López-Aranguren, J. Fraile, L. F. Vega and C. Domingo, *J. Phys. Chem. C*, 2012, **116**, 10150-10161.
27 S. Builes, P. López-Aranguren, J. Fraile, L. F. Vega and C. Domingo, *Energy & Fuels*, 2015, **29**, 3855-3862.
28 F. J. Blas and L. F. Vega, Molec. Phys., 1997, **92**, 135-150.
29 S. Builes and L. F. Vega, *Langmuir*, 2013, **29**, 199-206.
30 S. Minakata, Y. Okada, Y. Oderaotoshi and M. Komatsu, *Org. Lett.*, 2005, **7**, 3509-3512.
31 C. R. Dick and G. E. Ham, *J. Macromol. Sci. A*, 1970, **4**, 1301-1314.
32 T. Sakakura, J.-C. Choi and H. Yasuda, *Chem. Rev.*, 2007, **107**, 2365-2387.
33 K. Soga, S. Hosoda and S. Ikeda, *Die Makromolek. Chemie*, 1974, **175**, 3309-3313.
34 O. Ihata, Y. Kayaki and T. Ikariya, *Angew. Chem. Int. Ed.*, 2004, **43**, 717-719.
35 O. Ihata, Y. Kayaki and T. Ikariya, *Macromolec.*, 2005, **38**, 6429-6434.
36 E. Loste, J. Fraile, M. A. Fanovich, G. F. Woerlee and C. Domingo, *Adv. Mater.*, 2004, **16**, 739-744.
37 C. A. Garcia-Gonzalez, J. Saurina, J. A. Ayllon and C. Domingo, *J. Phys. Chem. C*, 2009, **113**, 13780-13786.
38 Z. N. Bacsik, N. Ahlsten, A. Ziadi, G. Zhao, A. E. Garcia-Bennett, B. N. Martin-Matute and N. Hedin, *Langmuir*, 2011, **27**, 11118-11128.
39 X. E. Hu, *Tetrahedron*, 2004, **60**, 2701-2743.
40 X. Wang and C. Song, *Catal. Today*, 2012, **194**, 44-52.
41 X. Wang, V. Schwartz, J. C. Clark, X. Ma, S. H. Overbury, X. Xu and C. Song, *J. Phys. Chem. C*, 2009, **113**, 7260-7268.
42 T. C. Drage, A. Arenillas, K. M. Smith and C. E. Snape, *Microp. Mesop. Mater.*, 2008, **116**, 504-512.
43 J. H. Drese, S. Choi, S. A. Didas, P. Bollini, M. L. Gray and C. W. Jones, *Microp. Mesop. Mater.*, 2012, **151**, 231-240.
44 W-J. Son, J-S. Choi and W-S. Ahn, *Microp. Mesop. Mater.*, 2008, **113**, 31-40.
45 A. Heydari-Gorji, Y. Yang and A. Sayari, *Energy & Fuels*, 2011, **25**, 4206-4210.
46 J. M. Rosenholm, A. Penninkangas and M. Linden, *Chem. Commun.*, 2006, 3909-3911.
47 J. C. Hicks, *PhD thesis*, Georgia Institute of Tecnology, 2007.
48 U. Ciesla, F. Schüth, *Microp. Mesop. Mater.*, 1999, **27**, 131-149.
49 K. B. Lee, M. G. Beaver, H. S. Caram and S. Sircar, I*nd. Eng. Chem. Res.*, 2008, **47**, 8048-8062.
50 Z. Bacsik, R. Atluri, A. E. Garcia-Bennett and N. Hedin, *Langmuir*, 2010, **26**, 10013-10024
51 D. J. N. Subagyono, Z. Liang, G. P. Knowles and A. L. Chaffee, *Chem. Eng. Res. Design*, 2011, **89**, 1647-1657
52 V. V. Mahajani and J. B. Joshi, *Gas Sep. Purification*, 1988, **2**, 50-64.
53 D. J. N. Subagyono, Z. Liang and G. P. Knowles, *Energy Procedia*, 2011, **4**, 839-843.
54 E. S. Sanz-Perez, M. Olivares-Marin, A. Arencibia, R. Sanz, G. Calleja and M. M. Maroto-Valer, Int. *J. Greenhouse Gas Control*, 2013, **17**, 366-375.
55 X. Wang, X. Ma, V. Schwartz, J. C. Clark, S. H. Overbury, S. Zhao, X. Xu and C. Song, *Phys. Chem. Chem. Phys.*, 2012, **14**, 1485-492.
56 A. Goeppert, M. Czaun, R. B. May, G. K. Surya Prakash, G. A. Olah and S. R. Narayanan, *J. Am. Chem. Soc.*, 2011, **133**, 20164-20167.
57 W. Li, S. Choi, J. Drese, M. Hornbostel, G. Krishnan, P. Eisenberger and C. Jones, *Chem. Sus. Chem.*, 2010, **3**, 899-903.
58 R. B. Vieira and H. O. Pastore, *Environ. Sci. Technol.*, 2014, **48**, 2472-2480.
59 C. H. Yu, C. H. Huang and C. S. Tan, *Aerosol Air Qual. Res*., 2012, **12**, 745-769.
60 X. Xu, C. Song, B. G. Miller, A. W. Scaroni, *Ind. Eng. Chem. Res.*, 2005, **44**, 8113-8119.
61 P. López-Aranguren, S. Builes, J. Fraile, L. F. Vega and C. Domingo, *Ind. Eng. Chem. Res.*, 2014, **53**, 15611-15619.
62 H-J. Kim, W. Chaikittisilp, K-S. Jang, S. A. Didas, J. R. Johnson, W. J. Koros, S. Nair and C. W. Jones, *Ind. Eng. Chem. Res.*, 2015, **54**, 4407-4413
63 S. Kim, J. Ida, V. V. Guliants and J. Y. S. Lin, *J. Phys. Chem. B*, 2005, **109**, 6287-6293.
64 Y. Belmabkhout and A. Sayari, *Energy & Fuels*, 2010, **24**, 5273-5278.

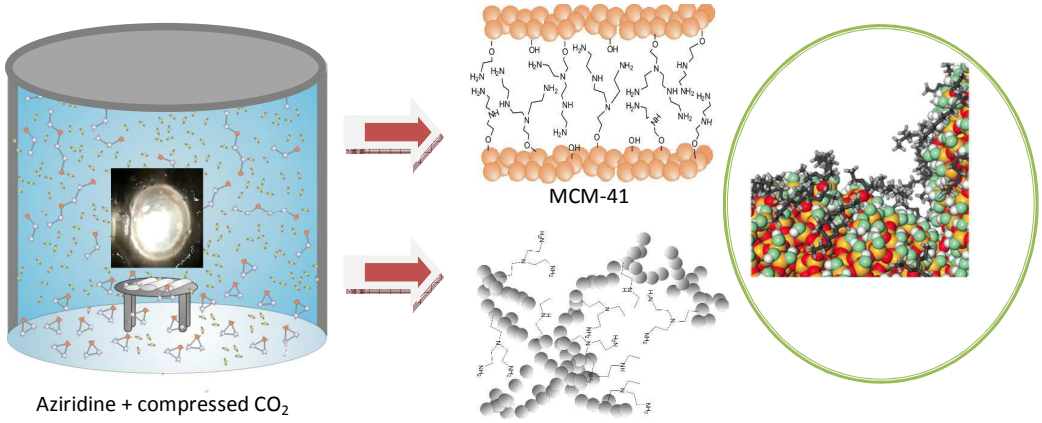

Experimental polymerization method of hyperbranched PEI based on the use of compressed CO_2